Proceedings of the 17th World Congress
The International Federation of Automatic Control
Seoul, Korea, July 6-11, 2008

Stabilization of a 2D-SpiderCrane Mechanism using Damping Assignment Passivity-based Control ⋆

Faruk Kazi * **Ravi N. Banavar** ** **Philippe Mullhaupt** ***
Dominique Bonvin ****

* *Indian Institute of Technology Bombay, Mumbai, India (e-mail: farukkazi@sc.iitb.ac.in).*
** *Indian Institute of Technology Bombay, Mumbai, India (e-mail: banavar@sc.iitb.ac.in).*
*** *Ecole Polytechnique Federale de Lausanne, CH-1015 Lausanne, Switzerland, (e-mail: philippe.muellhaupt@epfl.ch)*
**** *Ecole Polytechnique Federale de Lausanne, CH-1015 Lausanne, Switzerland, (e-mail: dominique.bonvin@epfl.ch)*

Abstract: In this paper, we present a modeling and control strategy for a cable suspended structure called the 'SpiderCrane'. By avoiding heavy mobile components, the design of this crane makes it particularly useful for work requiring high speeds. The modeling of such a multiple cable mechanism is challenging due to the number of constraints arising from cable interactions. From a control theoretical point of view, such mechanical systems are underactuated, which gives rise to challenging control issues.

Keywords: Underactuated mechanical systems; Passivity- based control; Cable operated robots; Holonomic constraints; Hamiltonian dynamics.

1. INTRODUCTION

Gantry cranes are all pervasive in the heavy engineering industry. Precise payload positioning by an overhead crane is difficult due to the fact that the payload may exhibit a pendulum-like swinging motion. This demands truly efficient control strategies. Motivated by this desire to achieve fast and precise payload positioning while minimizing swing, several researchers have proposed various control strategies for overhead crane systems. See Oh and Agrawal (2003); Fang et al. (2003); Liu et al. (2004). The problem with classical cranes is that the large inertia of the boom or the gantry limits rapid acceleration and deceleration since these may give rise to large inertial forces. For applications demanding fast weight handling a new crane design has been proposed by the Laboratory of Automatic Control at *École Polytechnique Fédérale de Lausanne*, see Buccieri et al. (2005). Its main feature is the absence of heavy mobile components. The heavy elements of the mechanical structure are fixed and the positioning is done by cables that carry the load. As a result, this crane can work at considerably higher speeds.

The control of mechanical systems in a nonlinear setting has received much attention in the past decade. Amongst the techniques developed, a general and promising one has been the interconnection and damping assignment passivity-based control (IDA-PBC) methodology. The idea here is to synthesize a controller that stabilizes the closed-loop system about a desired equilibrium and imparts certain characteristics to the closed-loop response by modifying the energy function and adding damping. In Acosta et al. (2005) and Ortega et al. (2002), IDA-PBC techniques are used to stabilize underactuated mechanical systems. The asymptotic stabilization of the classical ball-and-beam system and a novel inertia wheel pendulum is achieved through a new parametrization of the closed-loop inertia matrix. The IDA-PBC methodology is extended to the class of underactuated mechanical systems with kinematic constraints in Blankenstein (2002). Fujimoto et al. (2003), presented a coordinate transformation for trajectory tracking control of port-controlled Hamiltonian systems. The stabilization of a gantry crane system modeled with pulley dynamics leading to holonomic constraint using IDA-PBC is described in Banavar et al. (2006) and Kazi et al. (2007).

Still other researchers have proposed controllers synthesized from the differential flatness property of these systems to follow a specified trajectory, see Fliess et al. (1995); Maier and Woernle (2000); Kiss et al. (1999). Flat systems are equivalent to linear ones via a special type of feedback called endogenous. For such systems, the control inputs as well as all the internal state variables can be expressed in terms of a particular set of outputs (flat outputs) and a finite number of their time derivatives. This correspondence is useful for motion-planning tasks, where

⋆ This work was supported in part by the Laboratoire d'Automatique at *École Polytechnique Fédérale de Lausanne*, EPFL, Switzerland.

the parameterization of the flat outputs implies the one of the original state and inputs.

In this paper, we consider a planar version of the Spider-Crane consisting of two pylons as shown in Fig. 1. We refer to this mechanism as the 2D SpiderCrane. Our objective is twofold:

- Point-to-point transfer of the payload
- Minimize cable swing along the way.

We solve the problem using the IDA-PBC methodology.

The paper is organized as follows: Section 2 presents the dynamic model of the 2D SpiderCrane and formulates the problem. Section 3 provides a brief introduction to the IDA-PBC theory applied to such systems. We also discuss the IDA-PBC controller design for the robust stabilization of the 2D-SpiderCrane model under consideration. Simulation results for the controller designed with the IDA-PBC approach are discussed in Section 4. We wrap up the paper with some concluding remarks in Section 5.

2. SPIDERCRANE MODEL

Consider the 2D SpiderCrane shown in Fig. 1. The positioning of the load is done by adjusting the lengths l_1 and l_2. The model being underactuated and constrained by two holonomic constraints, it essentially captures all the control-theoretical perspectives of SpiderCrane discussed in Buccieri et al. (2005). Here, the position of the load is given by (x, y) with the load mass being m. The positions of the two motors are (x_a, y_a) and (x_b, y_b) with the corresponding rotary inertias taken as I_a and I_b. The ring has mass M and the position (x_R, y_R). The load is attached to the ring using a cable with fixed length of L_3. For the purpose of this study, we make the following assumptions:

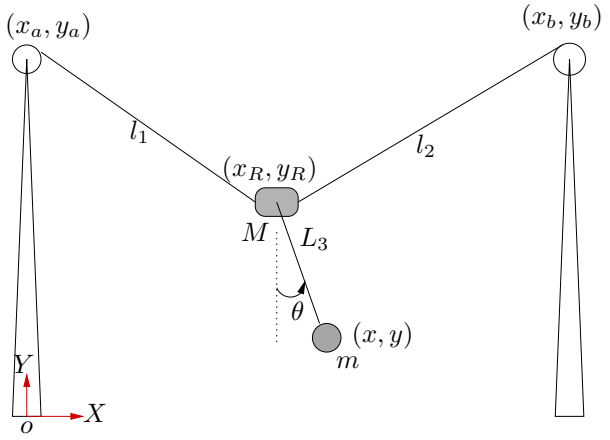

Fig. 1. 2D SpiderCrane mechanism

(1) The cable is massless and inelastic
(2) Dissipative forces on the cart and the winch are negligible
(3) Both the pylons are assumed to be at the same height.

2.1 Dynamics of 2D SpiderCrane

We first develop the dynamic model for the complete system to bring out some intrinsic system dynamics related issues. We begin with the following set of configuration variables

$$q = [x_R \quad y_R \quad \theta \quad l_1 \quad l_2]^T \tag{1}$$

where $\theta \in [0, 2\pi)$ denotes the payload angle about the vertical axis, $x_R \in \mathbb{R}^1$ denotes the ring position along the X-coordinate axis, $y_R \in \mathbb{R}^1$ denotes the ring position along the Y-coordinate axis and l_1, l_2 represent the cable lengths. The control $u \in \mathbb{R}^2$ is defined as $u = [F_1 \quad F_2]^T$ where F_1 and F_2 represent the control-force inputs acting on the first and second cable, respectively. Note that the rotary actuation of the winch translates to the winding/unwinding action of the cable. The control objective is to move the payload from any position $q_i = [x_{Ri} \quad y_{Ri} \quad \theta_i \quad l_{1i} \quad l_{2i}]^T$ to the desired position specified as $q_d = q_* = [x_{Rd} \quad y_{Rd} \quad \theta_d \quad l_{1d} \quad l_{2d}]^T$. At rest, the system has necessarily $\theta_d = 0$. The set of coordinates q as defined above is constrained by the following holonomic constraints:

$$\left.\begin{aligned} C_1(q) &= (x_R)^2 + (y_R - y_a)^2 - (l_1)^2 &&= 0 \\ C_2(q) &= (x_R - x_b)^2 + (y_R - y_b)^2 - (l_2)^2 &&= 0 \end{aligned}\right\} \tag{2}$$

The Lagrangian with the coordinate set q for the 2D SpiderCrane can be expressed as

$$\mathcal{L} = \frac{1}{2}\dot{q}^T M(q)\dot{q} - V(q) \tag{3}$$

where,

$$M(q) = \begin{bmatrix} M+m & 0 & mL_3\cos\theta & 0 & 0 \\ 0 & M+m & mL_3\sin\theta & 0 & 0 \\ mL_3\cos\theta & mL_3\sin\theta & {mL_3}^2 & 0 & 0 \\ 0 & 0 & 0 & I_a & 0 \\ 0 & 0 & 0 & 0 & I_b \end{bmatrix} \tag{4}$$

is the inertia matrix and the potential energy $V(q)$ is given as

$$V(q) = (M+m)gy_R - mgL_3\cos\theta. \tag{5}$$

The constraints (2) can be represented at the velocity level as $A^T(q)\dot{q} = 0$:

$$\begin{bmatrix} x_R & (y_R - y_a) & 0 & -l_1 & 0 \\ (x_R - x_b) & (y_R - y_b) & 0 & 0 & -l_2 \end{bmatrix} \begin{bmatrix} \dot{x}_R \\ \dot{y}_R \\ \dot{\theta} \\ \dot{l}_1 \\ \dot{l}_2 \end{bmatrix} = 0. \tag{6}$$

Note that $A(q)\lambda$ represents the constraint forces. The Lagrange multipliers $\lambda(t)$ are uniquely determined by the requirement that the constraints $A^T(q(t))\dot{q}(t) = 0$ have to be satisfied for all t. The annihilator of $A^T(q)$ is generated by the span of the columns of the matrix

$$S(q) \triangleq \begin{bmatrix} 0 & 0 & 1 \\ 0 & 1 & 0 \\ 1 & 0 & 0 \\ 0 & \dfrac{(y_R - y_a)}{l_1} & \dfrac{x_R}{l_1} \\ 0 & \dfrac{(y_R - y_b)}{l_2} & \dfrac{(x_R - x_b)}{l_2} \end{bmatrix}.$$

Hence, the admissible system motions lie in the range of $S(q)$ or, in other words, the vector $\dot{q}$ must be of the form

$\dot{q} = \eta S(q)$. Clearly for the following two configurations of the 2D SpiderCrane the Lagrange multipliers are not uniquely defined:

- the ring mass is at the first pulley with $l_1 = 0$
- the ring mass is at the second pulley with $l_2 = 0$.

Hence, these two points are excluded from our domain of operation.

2.2 Decoupled SpiderCrane Model

For the purpose of designing a control law, we consider the 2D SpiderCrane as a decoupled system as shown in Fig. 2. We first develop a control law based on the IDA-PBC

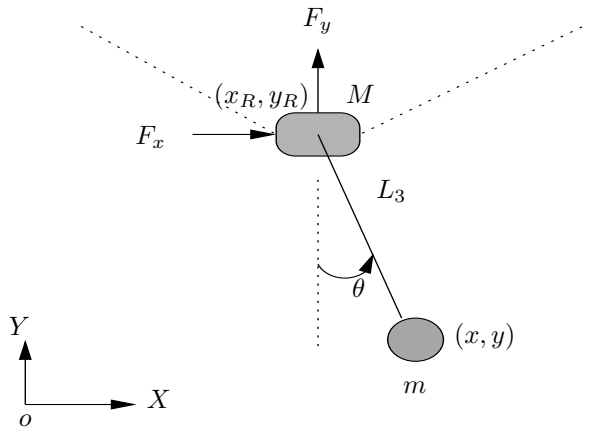

Fig. 2. 2D SpiderCrane gantry cart

methodology considering F_x and F_y as control inputs. We pose our problem as the control of the payload mass m suspended by a cable from the ring of mass M on which we have the two actuating forces F_x and F_y. Henceforth, we shall refer to this subsystem as the *gantry mechanism*. Given the trajectories of F_x and F_y, we then compute the cable tensions using the geometry of the problem.

The configuration variables for the gantry mechanism are $q = (x_R, y_R, \theta)^T$ and the Lagrangian can be expressed as

$$\mathcal{L}(q, \dot{q}) = \frac{1}{2}\dot{q}^T M(q)\dot{q} - V(q) \tag{7}$$

where,

$$M(q) = \begin{bmatrix} (M+m) & 0 & mL_3\cos\theta \\ 0 & (M+m) & mL_3\sin\theta \\ mL_3\cos\theta & mL_3\sin\theta & {mL_3}^2 \end{bmatrix}, \tag{8}$$

and $$V(q) = (M+m)gy_R - mgL_3\cos\theta. \tag{9}$$

The resulting Euler-Lagrange equations are:

$$\begin{aligned} F_x &= (M+m)\ddot{x}_R + (mL_3\cos\theta)\ddot{\theta} - (mL_3\sin\theta)\dot{\theta}^2 \\ F_y &= (M+m)\ddot{y}_R + (mL_3\sin\theta)\ddot{\theta} + (mL_3\cos\theta)\dot{\theta}^2 \\ &\quad +(M+m)g \\ 0 &= (mL_3\cos\theta)\ddot{x}_R + (mL_3\sin\theta)\ddot{y}_R + (m{L_3}^2)\ddot{\theta} \\ &\quad +mgL_3\sin\theta. \end{aligned}$$

We now consider to the Hamiltonian formulation using the Legendre transformation. The total energy of the system is represented by the Hamiltonian function

$$H(q, p) = \frac{1}{2}p^T M^{-1}(q)p + V(q) \tag{10}$$

where $q \in \mathbb{R}^n$ and $p \in \mathbb{R}^n$ are the generalized position and momenta, $M(q) = M^T(q) > 0$ is the inertia matrix, and $V(q)$ is the potential energy as defined in (8) and (9), respectively. If we assume that the system has no natural damping, the equations of motion can be written as

$$\begin{bmatrix} \dot{q} \\ \dot{p} \end{bmatrix} \begin{bmatrix} 0 & I_n \\ -I_n & 0 \end{bmatrix} \begin{bmatrix} \nabla_q H \\ \nabla_p H \end{bmatrix} + \begin{bmatrix} 0 \\ G(q) \end{bmatrix} u \tag{11}$$

with $u = [F_x \quad F_y]^T$. Note that for the 2D-SpiderCrane model, the matrix $G(q)$ takes the form

$$G(q) \begin{bmatrix} 1 & 0 \\ 0 & 1 \\ 0 & 0 \end{bmatrix}. \tag{12}$$

Its full-rank left annihilator $G^\perp$ (such that $G^\perp G = 0$) is given as $G^\perp = [0 \quad 0 \quad 1]$.

2.3 Pulley Dynamics

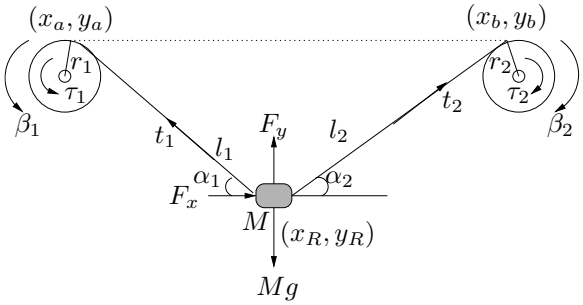

Fig. 3. Pulley-cable schematic

Consider the cable and pulley mechanism as shown in Fig. 3. Here β_i and τ_i represent the pulley angle and motor torque exerted by the motor, respectively, for the i^{th} pulley. We can express the forces acting on the cart in terms of the cable tensions t_1 and t_2 as follows:

$$\begin{bmatrix} F_x \\ F_y \end{bmatrix} = \begin{bmatrix} -\cos\alpha_1 & \cos\alpha_2 \\ \sin\alpha_1 & \sin\alpha_2 \end{bmatrix} \begin{bmatrix} t_1 \\ t_2 \end{bmatrix} + \begin{bmatrix} 0 \\ Mg \end{bmatrix}, \tag{13}$$

where α_1 and α_2 are as shown in Fig. 3. With the rotary inertias I_a and I_b for the first and the second pulley, the pulley dynamics read

$$\begin{bmatrix} I_a & 0 \\ 0 & I_b \end{bmatrix} \begin{bmatrix} \ddot{\beta}_1 \\ \ddot{\beta}_2 \end{bmatrix} = \begin{bmatrix} \tau_1 \\ \tau_2 \end{bmatrix} - r \begin{bmatrix} t_1 \\ t_2 \end{bmatrix}. \tag{14}$$

Here $r_1 = r_2 = r$ is the pulley radius. Also, the no-slip constraint on the i^{th} pulley gives $r\dot{\beta}_i = \dot{l}_i$. Combining (13) and (14) with the no-slip constraint, we can express the motor torques in terms of F_x and F_y as follows:

$$\begin{aligned} \begin{bmatrix} \tau_1 \\ \tau_2 \end{bmatrix} &= r \begin{bmatrix} \cos\alpha_1 & -\cos\alpha_2 \\ -\sin\alpha_1 & -\sin\alpha_2 \end{bmatrix}^{-1} \begin{bmatrix} F_x \\ F_y - Mg \end{bmatrix} \\ &\quad + r \begin{bmatrix} I_a & 0 \\ 0 & I_b \end{bmatrix} \begin{bmatrix} \ddot{l}_1 \\ \ddot{l}_2 \end{bmatrix} \qquad (\alpha_i > 0, i = 1, 2). \end{aligned} \tag{15}$$

Note that the above equation is subject to singularity, which occurs when the two cables lie along a straight line. Also note that $\ddot{l}_1$ and $\ddot{l}_2$ can be found from successive differentiation of the constraint equation (2).

3. IDA-PBC METHODOLOGY APPLIED TO 2D SPIDERCRANE

3.1 Basic Idea

In this section, we briefly discuss the IDA-PBC methodology developed in Ortega et al. (2002); Blankenstein et al. (2002). Motivated from (10), the desired (closed-loop) energy function is assumed to have the following form:

$$H_d(q,p) = \frac{1}{2}p^T {M_d}^{(-1)}(q)p + V_d(q) \tag{16}$$

where $M_d = {M_d}^T > 0$ and V_d represent the (to be defined) closed-loop inertia matrix and potential energy function, respectively. We will require that V_d have an isolated minimum at q_*, that is

$$q_* = \arg\min V_d(q). \tag{17}$$

The desired port-controlled Hamiltonian dynamics are taken of the form

$$\begin{bmatrix} \dot{q} \\ \dot{p} \end{bmatrix} = [\, J_d(q,p) - R_d(q,p) \,] \begin{bmatrix} \nabla_q H_d \\ \nabla_p H_d \end{bmatrix} \tag{18}$$

where the terms

$$\begin{aligned} J_d &= -{J_d}^T = \begin{bmatrix} 0 & M^{-1}M_d \\ -M_d M^{-1} & J_2(q,p) \end{bmatrix} \\ R_d &= {R_d}^T = \begin{bmatrix} 0 & 0 \\ 0 & GK_vG^T \end{bmatrix} \geq 0 \end{aligned}$$

represent the desired interconnection and damping structures, respectively. The matrix R_d is included to add damping into the system, which is expressed as,

$$u_{di} = -K_v G^T \nabla_p H_d \tag{19}$$

with $K_v = {K_v}^T > 0$. In the IDA-PBC method, the control effort consists of the following two basic steps:

- Energy shaping u_{es}, where we modify the total energy function of the system to assign the desired equilibrium $(q_*, 0)$
- Damping injection u_{di}, to achieve asymptotic stability.

Hence, the control input is given as

$$u = u_{es}(q,p) + u_{di}(q,p). \tag{20}$$

To obtain the energy shaping term, u_{es}, we express u in (11) from (20) and (19) and then use (18):

$$\begin{aligned} &\begin{bmatrix} 0 & I_n \\ -I_n & 0 \end{bmatrix} \begin{bmatrix} \nabla_q H \\ \nabla_p H \end{bmatrix} + \begin{bmatrix} 0 \\ G(q) \end{bmatrix} u_{es} \\ &= \begin{bmatrix} 0 & M^{-1}M_d \\ -M_d M^{-1} & J_2(q,p) \end{bmatrix} \begin{bmatrix} \nabla_q H_d \\ \nabla_p H_d \end{bmatrix}. \end{aligned} \tag{21}$$

While the first row of (21) is trivially satisfied, the second set of equations can be expressed as

$$Gu_{es} = \nabla_q H - M_d M^{-1} \nabla_q H_d + J_2 {M_d}^{-1} p. \tag{22}$$

If G is invertible, that is, if the system is fully actuated, we can uniquely solve for the control input u_{es} given any H_d and J_2. In the underactuated case, G is not invertible but only full column rank, and u_{es} can only influence the terms in the range space of G. This leads to the following set of constraint equations that must be satisfied for any choice of u_{es}:

$$G^\perp \{\nabla_q H - M_d M^{-1} \nabla_q H_d + J_2 {M_d}^{-1} p\} = 0 \tag{23}$$

where $G^\perp$ is a full-rank left annihilator of G, that is, $G^\perp G = 0$. Equation (23), with H_d given by (16), is a set of nonlinear PDEs with unknowns M_d and V_d, with J_2 a free parameter, and p an independent coordinate. If a solution for this PDE can be obtained, the resulting control law u_{es} reads

$$\begin{aligned} &u_{es} = \\ &(G^T G)^{-1} G^T (\nabla_q H - M_d M^{-1} \nabla_q H_d + J_2 {M_d}^{-1} p). \end{aligned} \tag{24}$$

The PDEs (23) can be separated into the terms that depend on p and the terms that are independent of p and can be equivalently written as

$$\begin{aligned} &G^\perp \{\nabla_q (p^T M^{-1} p) \\ &- M_d M^{-1} \nabla_q (p^T {M_d}^{-1} p) + 2J_2 {M_d}^{-1} p\} = 0 \end{aligned} \tag{25}$$

$$G^\perp \{\nabla_q V - M_d M^{-1} \nabla_q V_d\} = 0. \tag{26}$$

From here onwards, we refer to (25) as KE PDE for kinetic energy and (26) as PE PDE for potential energy. For further details on solving these PDEs, the interested reader is referred to Ortega et al. (2002).

3.2 Solving the PDEs for the 2D SpiderCrane

Since the desired equilibrium is a natural equilibrium of the system, we focus on shaping the potential energy of the system alone, thus leaving the kinetic energy unchanged. So we let $M_d = M$. In an attempt to influence the unactuated coordinate θ through modifying the interconnection structure we choose J_2 skew-symmetric and linear in p as follows

$$J_2 = k \begin{bmatrix} 0 & 0 & \dot{y}_R \\ 0 & 0 & -\dot{x}_R \\ -\dot{y}_R & \dot{x}_R & 0 \end{bmatrix}. \tag{27}$$

Clearly, it satisfies the KE PDE. We use $k \geq 0$ as a tuning parameter to influence the swing by changing interconnection structure. Providing this degree of freedom is the essence of IDA-PBC.

We now look for the solution of the PE PDE. With $G^\perp = (0 \quad 0 \quad 1)$, the potential energy PDE (26) takes the form $\nabla_{q_3} V - \nabla_{q_3} V_d = 0$, which is solved to give

$$V_d = -mgL_3 \cos\theta + \Phi(x_R, y_R). \tag{28}$$

Here, Φ is any arbitrary differentiable function whose selection is governed by the condition (17). If we choose Φ to be a quadratic function then we recover a PD like control law as in Fang et al. (2003). Here we use exponential function for the closed loop potential energy shaping. This choice is based on a comparatively large workspace of crane type systems compared to their counterpart- rigid robots. Exponential functions being steeper than quadratic, for a large deviation from the desired position the rate at which the system moves to the eqilibrium is faster as compared to the quadratic function. This yields

$$V_d(q) = -mgL_3\cos\theta + k_{p_x}(\exp(x_R - x_{R*}) - x_R) + k_{p_y}(\exp(y_R - y_{R*}) - y_R) \quad (29)$$

where $q_* = (x_{R*}, y_{R*}, 0)$ denotes the equilibrium configuration and $k_{p_x}, k_{p_y} > 0$ are used as tuning parameters. Clearly, with $\theta \in (-\frac{\pi}{2}, \frac{\pi}{2})$, the gradient and Hessian conditions for (17) are satisfied.

To compute the final control law, we first determine the energy-shaping term u_{es} from (24), which, in this case, takes the form

$$u_{es} = \begin{bmatrix} -k_{p_x}(\exp(x_R - x_{R*}) - 1) \\ (M+m)g - k_{p_y}(\exp(y_R - y_{R*}) - 1) \end{bmatrix} + \begin{bmatrix} k\dot{y}_R\dot{\theta} \\ k\dot{x}_R\dot{\theta} \end{bmatrix}. \quad (30)$$

The controller design is completed with the damping injection term (19), which yields

$$u_{di} = -K_v G^T \dot{q} = -\begin{bmatrix} k_a\dot{x}_R + k_b\dot{y}_R \\ k_b\dot{x}_R + k_c\dot{y}_R \end{bmatrix}.$$

We consider K_v to be a symmetric and positive definite matrix of the form $K_v = \begin{bmatrix} k_a & k_b \\ k_b & k_c \end{bmatrix}$. The role of the tuning parameters has a clear interpretation. The gains k_{p_x}, k_{p_y} are like proportional gains and act on the errors in the configuration variables, which contributes to the proportional-like term in the control law. The K_v terms acts on the derivatives of the error and injects damping into the system. The other terms in the final control law also assume a nice physical interpretation

$$u = \underbrace{\begin{bmatrix} -k_{p_x} & 0 \\ 0 & -k_{p_y} \end{bmatrix}\begin{bmatrix} \exp(x_R - x_{R*}) - 1 \\ \exp(y_R - y_{R*}) - 1 \end{bmatrix}}_{\text{proportional-like}} + \underbrace{\begin{bmatrix} 0 \\ (M+m)g \end{bmatrix}}_{\text{gravity term}} - \underbrace{\begin{bmatrix} k_a & k_b \\ k_b & k_c \end{bmatrix}\begin{bmatrix} \dot{x}_R \\ \dot{y}_R \end{bmatrix}}_{\text{damping}} + \underbrace{\begin{bmatrix} 0 & k\dot{\theta} \\ -k\dot{\theta} & 0 \end{bmatrix}\begin{bmatrix} \dot{x}_R \\ \dot{y}_R \end{bmatrix}}_{\text{gyroscopic}}. \quad (31)$$

4. SIMULATION STUDY

The system parameters are taken as $M = 0.5$ kg for ring mass and $m = 1$ kg for payload mass to match the laboratory-scale model of the SpiderCrane. For the simulations, the tuning parameters were selected as $k_a = 6, k_b = 0, k_c = 20, k_{p_x} = 3, k_{p_y} = 7$. The desired equilibrium position is chosen as $[x_{R*} \quad y_{R*} \quad \theta_*] = [0.5 \quad 1.0 \quad 0]$. Fig. 4 illustrates the controller performance with initial conditions of the swing angle as 10 deg, $x_R = 0.7$ m, $y_R = 0.7$m. The effect of gyroscopic forces on cable swing by changing the interconnection structure is visible in Fig. 5. Here, we use all parameters same as in the simulation for Fig. 4 except for k, the tuning parameter in matrix J_2. Compare the swing experienced by the ring trajectory in (x_R, y_R) sub-plot with the payload trajectory in (x, y) sub-plot in these two figures. Clearly, the IDA-PBC control law provides an ability to influence the payload swing by changing interconnection structure. We further demonstrate the controller performance with an initial condition of 30 deg in Fig. 6 to emphasize a dominantly nonlinear case of a comparatively large swing angle. Here, all other parameters are kept the same as in the case of Fig. 4.

The last simulation depicts the robustness property of the IDA-PBC controller (Fig. 7). Here we change the cart mass to 1.5 kg and the payload mass to 3 kg while keeping the same controller parameters as in Fig. 4. The system response does not change significantly but the control effort is observed to be significantly larger.

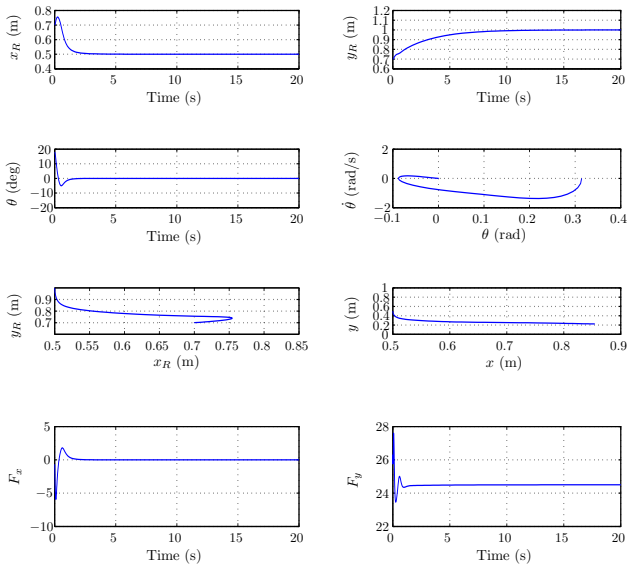

Fig. 4. Simulation for initial swing $\theta = 10°$, $k = 10$.

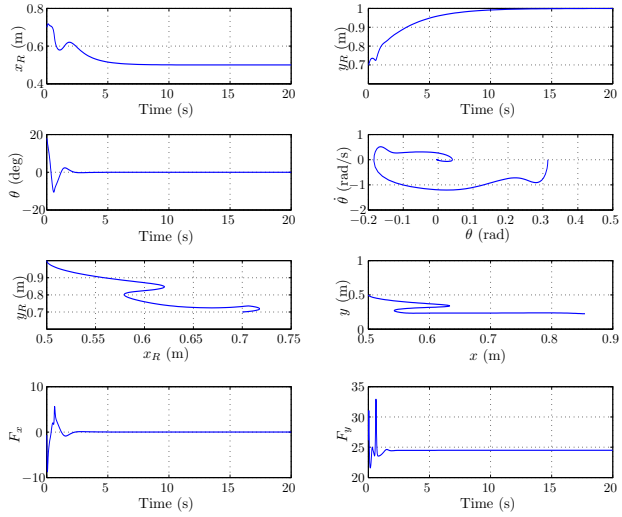

Fig. 5. Simulation for initial swing $\theta = 10°$ but $k = 35$.

5. CONCLUSIONS

We have presented a controller design procedure for a 2-dimensional version of the SpiderCrane model. The design procedure is based on the IDA-PBC mehtodology wherein we shaped the potential energy of the system

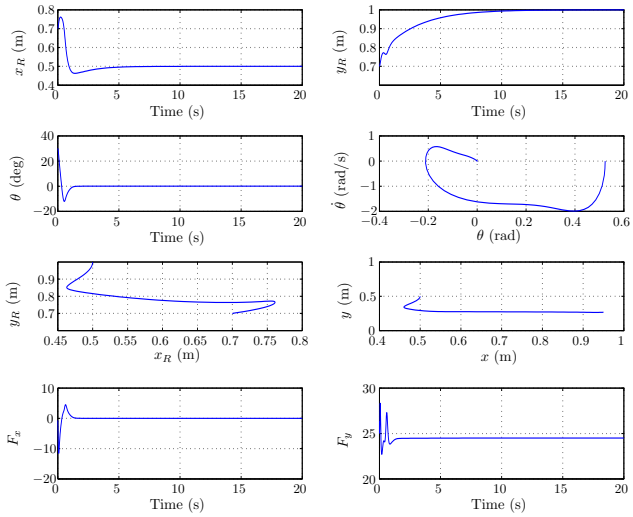

Fig. 6. Simulation for larger initial swing of $\theta = 30°$, $k = 10$.

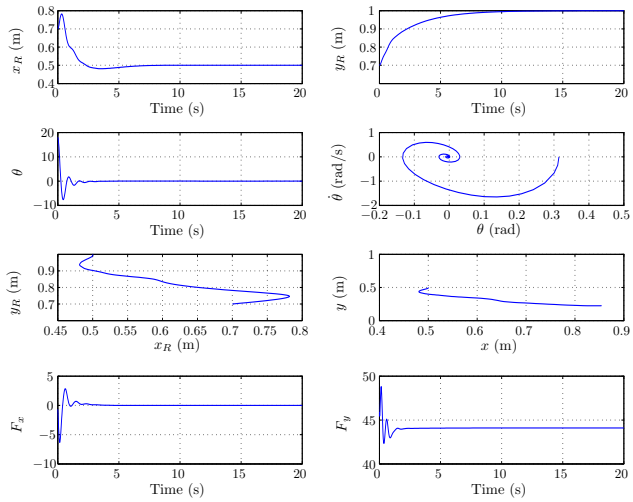

Fig. 7. Simulation results for robustness.

using exponential function. We have also exploited the freedom in the interconnection matrix J_2 in the IDA-PBC framework to influence the cable sway which is an unactuated coordinate. The resulting control law, as observed in the simulations, was found to be performing well for the control objective of point-to-point control with swing minimization. The performance of the nonlinear controller for the large swing angle, beyond the linearizable region, is analyzed by simulation. The robustness inherent to passivity-based controllers was observed in the simulations. Future efforts will focus on extending this methodology to the 3-dimensional SpiderCrane mechanism.

6. ACKNOWLEDGMENTS

We thank Romeo Ortega for many helpful discussions on the IDA-PBC technique.

REFERENCES

J. A. Acosta, R. Ortega, A. Astolfi, and A. D. Mahindrakar. Interconnection and damping assignment passivity-based control of mechanical systems with underactuation degree one. *IEEE Trans. on Automatic Control*, 50(12):1936–1955, 2005.

R. Banavar, F. Kazi, R. Ortega, and N. S. Manjarekar. The IDA-PBC methodology applied to a gantry crane. In *Proceedings of the Mathematical Theory of Networks and Systems*, pages 143–147, Kyoto, Japan, 2006.

G. Blankenstein. Matching and stabilization of constrained systems. In *Proceedings of the Mathematical Theory of Networks and Systems*, Notre Dame, Indiana, 2002.

G. Blankenstein, R. Ortega, and A. J. van der Schaft. The matching conditions of controlled Lagrangians and IDA-passivity based control. *International Journal of Control*, 75(9):645–665, 2002.

D. Buccieri, Ph. Mullhaupt, and D. Bonvin. SpiderCrane Model and Properties of a Fast Weight Handling Equipment. In *The* 16^{th} *IFAC world congress*, Prague, 2005.

Y. Fang, W. E. Dixon, D. M. Dawson, and E. Zergeroglu. Nonlinear Coupling Control Laws for an Underactuated Overhead Crane System . *IEEE Trans. on Mechatronics*, 8(3):418–423, 2003.

M. Fliess, J. Levine, Ph. Martins, and P. Rouchon. Flatness and defect of non-linear systems: introductory theory and examples . *International Journal of Control*, 61 (6):1327–1361, 1995.

K. Fujimoto, K. Sakurama, and T. Sugie. Trajectory tracking control of port-controlled Hamiltonian systems via generalized canonical transformations. *Automatica*, 39(12):2059–2069, 2003.

F. Kazi, R. Banavar, R. Ortega, and N. S. Manjarekar. Point-to-Point control of a gantry crane: A combined flatness and IDA-PBC strategy. In *Proceedings of the European Control Conference*, pages 5815–5820, Kos, Greece, 2007.

B. Kiss, J. Levine, and Ph. Mullhaupt. Modelling, flatness and simulation of a class of cranes . *Periodica Polytechnica*, 43(3):215–255, 1999.

D. Liu, W. Guo, J. Yi, and D. Zhao. Passivity-Based-Control for a Class of Underactuated Mechanical Systems . In *Proceedings of the 2004 International Conference on Intelligent Mechatronics and Automation*, pages 50–54, Chengdu, China, 2004.

T. Maier and C. Woernle. Dynamics and Control of a Cable Suspension Manipulator. In *The* 9^{th} *German-Japanese seminar on Nonlinear Problems in Dynamical systems-Theory and Applications*, Straelen, Germany, 2000.

S. R. Oh and S. K. Agrawal. Cable suspended planar parallel robots with redundant cables: Controllers with positive cable tensions. *IEEE International Conference on Robotics and Automation*, 3:3023–3028, September 2003.

R. Ortega, M. W. Spong, F. Gomez-Estern, and G. Blankenstein. Stabilization of a Class of Underactuated Mechanical Systems via Interconnection and Damping Assignment. *IEEE Trans. on Automatic Control*, 47(8):1218–1233, 2002.